Decline and recovery of pelagic acoustic backscatter following El Niño events in the Gulf of California, Mexico

Elan J. Portner[a,*], Kelly J. Benoit-Bird[b], Elliott L. Hazen[c], Chad M. Waluk[b], Carlos J. Robinson[d], Jaime Gómez-Gutiérrez[e], William F. Gilly[a]

[a] *Hopkins Marine Station of Stanford University, Pacific Grove, CA, USA*

[b] *Monterey Bay Aquarium Research Institute, Moss Landing, CA, USA*

[c] *NOAA Southwest Fisheries Science Center, Monterey, CA, USA*

[d] *Instituto de Ciencias del Mar y Limnología, Universidad Nacional Autónoma de México, D.F., Mexico*

[e] *Centro Interdisciplinario de Ciencias Marinas, Instituto Politécnico Nacional, La Paz, B.C.S., Mexico*

*Corresponding author at current address:

Scripps Institution of Oceanography, UCSD

8622 Kennel Way, La Jolla, CA, USA 92037, E-mail: eportner@ucsd.edu (E.J. Portner)

A B S T R A C T

Climatic variability exerts enormous pressures on the structure and function of open ocean ecosystems. Although the responses of primary producers and top predators to these pressures are being increasingly well-documented, little is known about how midtrophic communities respond to oceanographic and climatic variability. We address this knowledge gap through a study of the effects of El Niño Southern Oscillation (ENSO) and local environmental conditions on acoustic proxies of the midtrophic community in the Gulf of California, Mexico. We quantified the intensity and distribution of nighttime acoustic backscatter (120 kHz) in the upper 200 m of the water column during 10 oceanographic cruises (2007–2017) and described its response to environmental variability using generalized additive models. ENSO conditions were the strongest drivers of variability in backscatter after accounting for seasonal increases in backscatter with sea surface temperature and chlorophyll-*a* concentration. Acoustic backscatter in the central Gulf of California decreased significantly during the positive phase of ENSO. Following El Niño events in 2009-10 and 2015-16, mean backscatter declined by an order of magnitude and remained depressed for more than two years before recovering to pre-El Niño levels. Scattering layer density increased with total backscatter, likely an influential factor determining prey availability for pelagic predators. Our findings demonstrate large and sustained impacts of El Niño on the midtrophic community in the Gulf of California and further highlight the need to better understand the responses of midtrophic communities to environmental variability.

Keywords:

Hydroacoustic

Backscattering layers

Midtrophic communities

Generalized additive models

El Niño Southern Oscillation

Highlights

- Timeseries of acoustic backscatter as a proxy for midtrophic biomass in the Gulf of California.
- ENSO explained more variability than regional temperature or chlorophyll concentration.
- Backscatter decreased significantly during the positive phase of ENSO (El Niño).
- Mean backscatter took more than two years to recover to pre-El Niño levels.

1. Introduction

Over the past century, marine capture fisheries production has quadrupled (FAO, 2016) and human activities, particularly greenhouse gas emissions, have contributed to warming of the global ocean by ~0.6 ºC (Levitus et al., 2001; Gleckler et al., 2016). Our observations and understanding of the ways pelagic organisms respond to these pressures are heavily skewed toward primary producers and top predators. On average, the global biomass of primary producers in the ocean is decreasing in response to ocean warming (Polovina et al., 2008; Boyce et al., 2010; Rykaczewski and Dunne, 2011). Predatory fishes, birds, and mammals are also rapidly changing in abundance and distribution, often in response to the combined pressures of fishing and warming (Veit et al., 1997; Lewison et al., 2004; Polovina et al., 2009; Hazen et al., 2013; Woodworth-Jefcoats et al., 2015).

Food-web models suggest anthropogenic pressures on pelagic ecosystems are not simply additive, but that top-down and bottom-up effects of these pressures may be modulated by the midtrophic organisms in pelagic food webs (Woodworth-Jefcoats et al., 2015; Choy et al., 2016). Midtrophic biomass is composed of diverse fishes, crustaceans, gelatinous organisms, and cephalopods, many of which aggregate into relatively dense communities that are observable as acoustic scattering layers within the upper 1000 m of the water column (Kloser et al., 2009; Ritz et al., 2011; Klevjer et al., 2016). In addition to linking production at the base of food webs (phytoplankton) to top predators, midtrophic organisms help to link surface to deep pelagic habitats through diel vertical migration (Ducklow et al., 2001; Ambriz-Arreola et al., 2017). Daily movement between nighttime feeding grounds at the ocean surface and daytime refuge at depth actively contributes to carbon sequestration as part of the pelagic biological pump. This ‘mesopelagic-migrant pump’ component accounts up to 50% of the total downward carbon

72 transport (Zhang and Dam, 1997; Hidaka et al., 2001; Schukat et al., 2013), and is surpassed only
73 by the gravitational pump component with respect to carbon export rates (Boyd et al., 2019).
74 Changes in the abundance of midtrophic organisms are thus expected to impact both the
75 ecological and biogeochemical functions of pelagic ecosystems. Variability in the biomass of
76 midtrophic organisms has been observed at coarse spatial scales (e.g. across ocean basins, Kloser
77 et al., 2009; Irigoien et al., 2014) and fine temporal scales (e.g. days to weeks; McClatchie and
78 Dunford, 2003), but there are few time series that can demonstrate the responses of these
79 communities to large-scale environmental variability over a prolonged period (Godø et al., 2014;
80 Proud et al., 2017; Koslow et al., 2018). As such, the responses of midtrophic communities to
81 environmental variability represents a critical gap in our understanding of pelagic ecosystem
82 dynamics.
83 Climatic conditions define baseline ocean heat content and atmosphere interactions and
84 mitigate seasonal oceanographic variability in pelagic habitats. El Niño Southern Oscillation
85 (ENSO) is a recurring climate pattern that describes heat content distribution in the tropical
86 Pacific Ocean and is quantified by the multivariate ENSO Index (MEI.v2, NOAA Physical
87 Sciences Laboratory, https://psl.noaa.gov/enso/mei/). Over the past four decades (1980-2020),
88 there have been eight El Niño events (positive ENSO extremes defined as at least five
89 consecutive months of MEI.v2 > 0.5), characterized by a major redistribution of heat content
90 from west to east – in 1982-83, 1986-87, 1991-94, 1997-98, 2002-03, 2006-07, 2009-10, and
91 2015-16 (https://psl.noaa.gov/enso/mei/). Regional conditions in the Gulf of California, Mexico,
92 a marginal sea located in the northeastern subtropical Pacific, are greatly impacted by the water
93 masses available for exchange at the mouth of the gulf (Herrera-Cervantes et al., 2007; Staines-
94 Urías et al., 2009; Portela et al., 2016). During El Niño events, tropical water masses become

more available for exchange (Baumgartner et al., 1985; Frawley et al., 2019) and the Gulf of California experiences increased sea surface temperature (SST) and subsurface warming (Lluch-Cota et al., 2007, 2010), as well as overall diminution and redistribution of phytoplankton biomass (Kahru et al., 2004; Robinson et al., 2016).

Strong El Niño events (MEI.v2 > 1) in 1982-83 and 1997-98 were associated with changes in abundance of anchovy, sardines, and zooplankton in the Gulf of California (Lavaniegos et al., 1989; Lavaniegos-Espejo and Lara-Lara, 1990; Sánchez-Velasco et al., 2004; Velarde et al., 2013, 2015; Petatán-Ramírez et al., 2019; Arreguín-Sánchez et al., 2021) and a range of responses was observed for predators at higher trophic levels in conjunction with events in 1997-98 and 2009-10. Elegant terns (*Thalasseus elegans*) failed to nest on their specific site on Isla Raza in the central Gulf of California and instead shifted north to nest well outside the Gulf (Velarde et al., 2013, 2015). Humboldt squid (*Dosidicus gigas*) show a more complex response: squid biomass redistributed from neritic to pelagic habitats; lifespan was severely reduced (> 1.5 years to < 0.5 year); and size at maturity was reduced (> 60 cm mantle length (ML) and 10 kg body mass to < 20 cm ML and 0.1 kg body mass) (Hoving et al., 2013; Robinson et al., 2016). Although both predators recovered rapidly after the strong El Niño of 1997-98, recovery after the 2009-10 event was erratic and further hindered by the strong 2015-16 El Niño (Velarde, *pers. comm.;* Frawley et al., 2019). Prey biomass and density are both important determinants of habitat selection and foraging success for marine predators (Benoit-Bird, 2009; Hazen and Johnston, 2010; Benoit-Bird et al., 2013; Carroll et al., 2017), and prey availability may mitigate predator responses to climatic events. However, the responses of midtrophic prey in the Gulf of California to El Niño events are poorly described and represent a critical gap in our understanding of the effects of environmental variability on pelagic food webs.

To estimate the response of midtrophic communities to environmental variability, we quantified acoustic backscatter intensity and distribution in the central Gulf of California based on ten oceanographic surveys carried out between January 2007 and June 2017. This period included warm- and cool-season sampling as well as three El Niño events (2006-07, 2009-10, and 2015-16). The goals of the present study were 1) to assess sensitivity of nighttime acoustic backscatter in the upper 200 m of the water column to ENSO conditions, sea surface temperature, and sea surface chlorophyll-*a* concentrations, and 2) to determine the time scales over which El Niño events impacted the midtrophic assemblages that contribute to backscatter. This work provides unique insight into the relative impacts of local environmental and ENSO conditions on midtrophic biomass inferred from acoustic backscatter in the Gulf of California and may help us understand how projected increases in the frequency and intensity of El Niño events will affect midtrophic organisms in the eastern Pacific Ocean.

2. Materials and methods

2.1. Acoustic sampling and data processing

Acoustic data were recorded from the central Gulf of California (~26–29.5º N, Fig. 1) on 10 oceanographic cruises aboard the R/V El Puma (Universidad Nacional Autónoma de México) during relatively "warm" (June – October) and "cool" seasons (November – May) between January 2007 and June 2017 (Table S1). Each cruise lasted approximately three weeks (with effective acoustic survey durations between 6 –18 days) and covered an average of ~3600 km of transect at speeds of 7– 26 km h^{-1} (4 –14 kts) (Table S1). Acoustic data were collected using a 120 kHz split-beam scientific echosounder (Simrad ES60 echosounder, Simrad ES120-7C, 7-degree split-beam transducer). Pulse lengths (0.256 – 1.054 ms) and power settings of the

transducer (200-500 W) varied by cruise and are listed in Table S1. The transducer was mounted on the end of a steel pole that was extended into the water through a moon pool in the center of the ship to a depth of 4 m below the sea surface. All reported depths are ranges (in meters) from the transducer. Field calibrations of the transducer were performed periodically throughout the study using a reference sphere as described in Gómez-Gutiérrez and Robinson (2006). Calibrations indicated no change in system performance. Constant, nominal calibration values were used for all data to allow relative changes in acoustic backscatter to be robustly assessed.

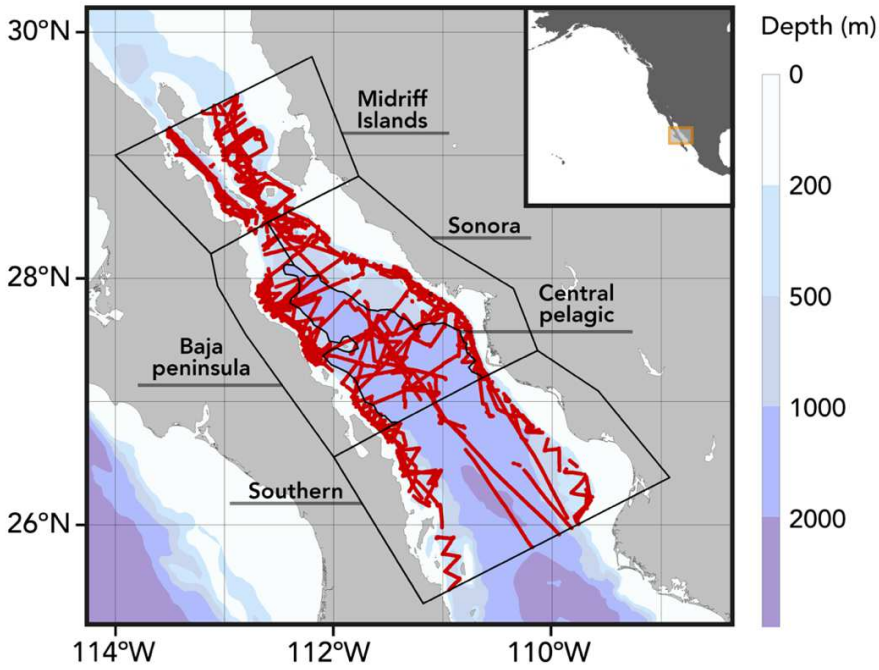

Fig. 1. Bathymetric map of the central Gulf of California, Mexico showing nighttime cruise tracks over seafloor depths > 200 m from all ten cruises combined (red lines). Regions used for monthly environmental covariate averages and NASC anomaly calculations are outlined in black. Nighttime cruise tracks from each oceanographic cruise are given in Fig. S1. The study area is depicted as an orange box in the inset map of North America.

154 Acoustic data were processed in Echoview version 10 (Echoview, 2019) using built-in
155 background and transient noise removal procedures. ES60 data were corrected to remove the
156 triangle-wave error in Echoview following Keith et al. (2005). To account for variability in pulse
157 lengths among cruises, all data were resampled to 1000 samples per ping. To minimize
158 variability introduced by the inclusion of strictly shelf-associated species, we only included data
159 collected in waters with sea floor depths > 200 m as determined by automatic bottom detection
160 procedures in Echoview and verified by manual examination. Analyses were limited to data
161 collected between 10 and 200 m depth (hereafter, "upper 200 m"), representing data with a
162 signal-to-noise ratio that enabled robust ecological interpretation of echoes. This includes
163 organisms that are resident in the upper 200 m, as well as those that migrate into this depth range
164 at night from daytime habitats in the mesopelagic zone (200 – 1000 m) (Gómez-Gutiérrez and
165 Robinson, 2006; Benoit-Bird and Gilly, 2012). We therefore limited analyses to nighttime
166 samples as a proxy for prey available to predators that feed between the surface and mesopelagic
167 depths (Benoit-Bird and Au, 2003; Klevjer et al., 2016). "Nighttime" was defined based on
168 estimates of when vertically migrating animals end their diel ascent relative to local sunset times
169 (i.e. start of night) and begin their diel descent relative to local sunrise times (i.e. end of night)
170 (Table S1; Cade and Benoit-Bird, 2015). The cruise tracks of nighttime acoustic surveys in
171 waters with sea floor depths > 200 m for each cruise are given in Fig. S1. Acoustic data were
172 integrated per km of cruise track using a minimum Sv threshold of -125 dB.
173
174 *2.2. Acoustic metrics of midtrophic community abundance and density*
175 Metrics of acoustic backscatter were quantified to estimate variability in the total
176 abundance and density of midtrophic organisms in the water column, both of which affect their

availability to predators. The relative abundance of midtrophic organisms was estimated as the nautical area backscattering coefficient (NASC, sA, m^2 nmi^{-1}, MacLennan et al., 2002) per kilometer of cruise track. To examine variability in the distribution of backscatter in the upper 200 m, features of scattering layers were defined as follows. First, data from each ping were filtered for bins with mean volume backscattering strength (MVBS, Sv, dB re 1 m^{-1}, hereafter dB, MacLennan et al., 2002) in the 90th percentile, allowing for identification of the shallowest and deepest depths of these bins per ping. The averages of these depths were used to define the vertical edges of a scattering layer's "width" (expressed in meters) over each kilometer of cruise track (Fig. 2). NASC was integrated between these edges ("wNASC", m^2 nmi^{-1}) and divided by layer width to obtain an estimate of "density" within the scattering layer. When log-transformed, these layer density values are proportional to MVBS. We examined the relationships between layer width and wNASC, as well as layer density and total NASC to describe the vertical distribution of backscatter within the upper 200 m.

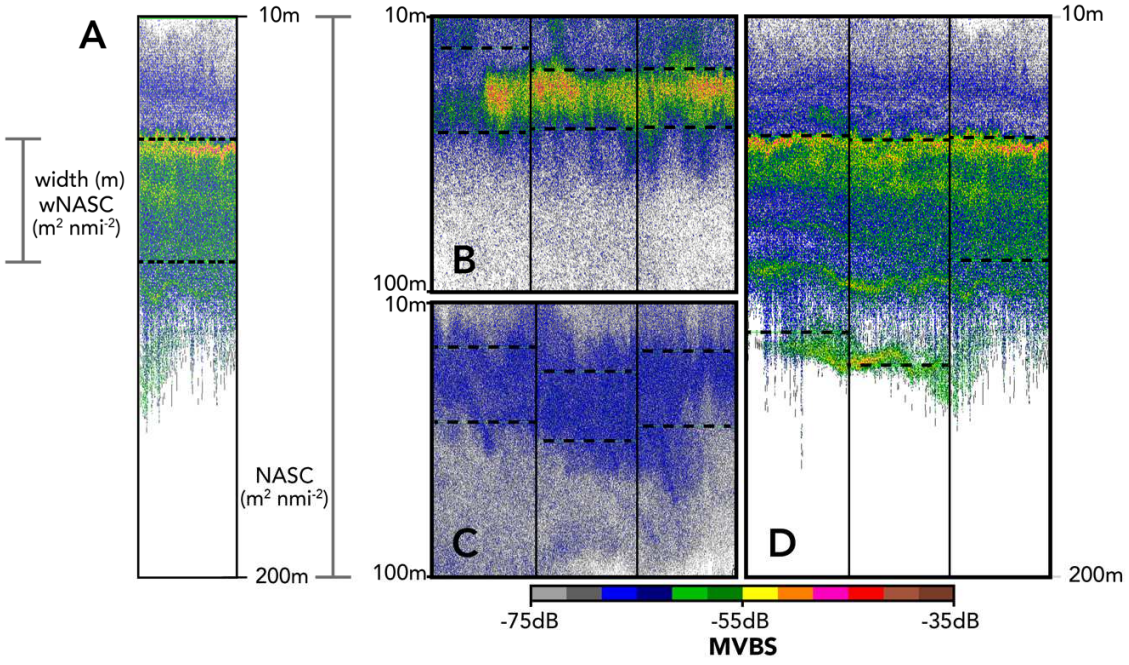

Fig. 2. Visual representation of acoustic metric definitions and variability in acoustic backscatter in the Gulf of California recorded during ten oceanographic surveys carried out from January 2007 to July 2017. (A) Schematic illustrating the definitions of scattering-layer width and integrated wNASC that were used for estimating the abundance and distribution of midtrophic organisms. Representative echograms in the upper water column from the cool season (B, February 2014) and (C, March 2010) and the warm season (D, August 2014). Panels illustrate differences in MVBS (dB) for cruises with relatively high (B, D) and low NASC (C). Panels B-D each display 3 km of cruise track (km delimited by black vertical lines) collected at night in waters with sea floor depths $\geq$ 200 m. Horizontal dashed lines indicate the average vertical edges of acoustic scattering layers per kilometer of cruise track as defined in *Methods section 2.2*. Increased vertical structure (e.g., multiple layers at different depths) of acoustic backscatter decreases the measured density of a defined layer (Panels B and D have similar NASC, but density in B is two- to four-fold higher than in D).

Although we were unable to directly sample and identify the scattering organisms with trawls or other methods during the acoustic surveys, we contextualize backscatter measurements by comparing them to observations of spatiotemporal trends in the size structure and composition of midtrophic organisms in the Gulf of California (Domínguez-Contreras et al., 2012; Robinson et al., 2014; García-Fernández et al., this issue). We did not explicitly filter out signals from larger predators, and we assumed that most organisms scattering sound at 120 kHz represented midtrophic organisms ~0.5 – 20cm in length, including both mesozooplankton and micronekton (Irigoien et al., 2014; Proud et al., 2017). Hereafter, organisms that contribute to acoustic backscatter at 120 kHz are simply referred to as "midtrophic organisms".

All analyses were performed using packages in the R statistical environment (R Core Team, 2020). NASC and wNASC were log-transformed to better match the theoretical assumptions of the statistical tests applied to these data. To examine variability in NASC among cruises, NASC anomalies were quantified as deviations from the mean log-transformed NASC per oceanographic region across our study period (Fig. 1). Regions were defined based on oceanographic and biogeographic characteristics following Portner et al. (2020) to account for diverse habitats within our study area that may be expected to support distinct midtrophic communities. Briefly, the Midriff Islands region is separated from the rest of the gulf by a sill and supports distinct taxa (e.g. Brinton et al., 1986; Alvarez-Borrego and Ruben Lara-Lara, 1991; Robison, 1972); the Southern region was distinguished from the central Gulf based on biogeographic boundaries (e.g. Round, 1967; Brinton et al., 1986); and the three central regions (Baja Peninsula, Sonora, and Central Pelagic) were distinguished by the 1000 m isobath.

225 *2.3. Environmental covariates describing pelagic habitat conditions in the Gulf of California*

226 Sea surface temperature (SST) and chlorophyll-*a* concentration (Chl-*a*, as a proxy for
227 standing biomass of phytoplankton) were used to describe the environmental conditions of
228 pelagic habitats of the Gulf of California. Observation-based SST (monthly, 0.25º x 0.25º) and
229 Chl-*a* (monthly, 4 x 4 km) products were accessed from the E.U. Copernicus Marine Service
230 Information (http://marine.copernicus.eu). In addition, NOAA's Multivariate ENSO Index
231 (MEI.v2) (Wolter and Timlin, 1993) was used to provide a more global environmental correlate,
232 with bimonthly MEI values obtained from the NOAA Earth Systems Research Laboratory
233 (https://www.esrl.noaa.gov/psd/enso/mei/table.html).

234 Oceanographic conditions at the time of data collection do not necessarily capture the
235 environmental history that would influence recruitment, growth, movement, and reproduction
236 that ultimately determine the biomass and taxonomic composition of midtrophic communities.
237 To address the variable temporal scales of interest and spatiotemporal resolutions of our
238 environmental datasets we calculated monthly regional averages of SST and Chl-*a* (Fig. 1, Fig.
239 3). Regional averages of SST over zero, three, and twelve-month periods prior to data collection
240 were thus considered to capture effects of intra-annual variability in SST, as well as inter-annual
241 temperature trends. Nine- and twelve-month averages of MEI.v2 were considered to examine the
242 effects of larger-scale climatic history at temporal scales that would describe the dominant water
243 masses entering the mouth of the gulf and their effects on water-column structure (Baumgartner
244 et al., 1985; Frawley et al., 2019). Chl-*a* concentrations were assumed to be ecologically
245 important at shorter temporal scales than physical environmental conditions. Croll et al. (2005)
246 demonstrated a 4 – 6 month lag between peak Chl-*a* and peak krill biomass in an eastern Pacific

upwelling system off California, and we therefore considered three- and six-month averages of Chl-*a* as an estimate of integrated food availability for midtrophic organisms.

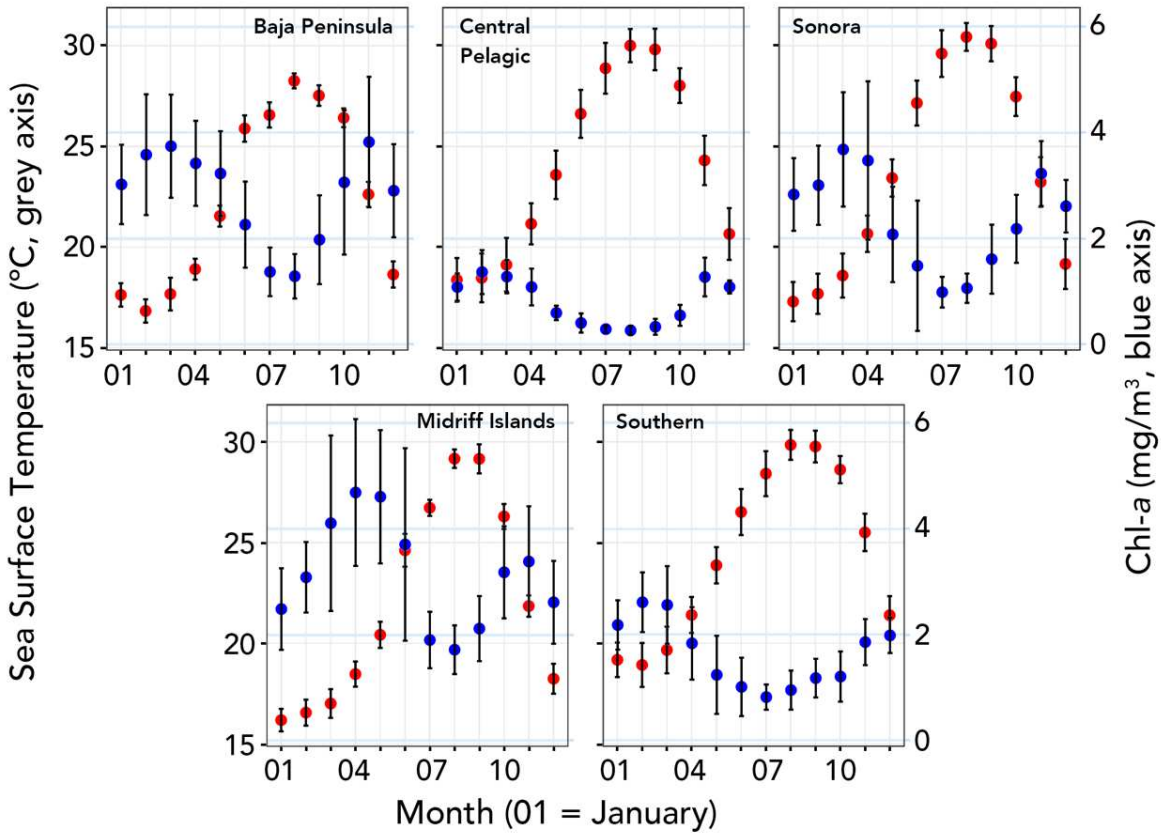

Fig. 3. Monthly averages of sea surface temperatures (red) and chlorophyll-*a* concentrations (Chl-*a*, blue) in the Gulf of California recorded during January 2006 – October 2017 from each biogeographic region shown in Fig. 1 (black whiskers represent standard deviations).

The principal source of interannual climate variability in Gulf of California is the changing intensity of equatorial circulation associated with ENSO (Baumgartner et al., 1985; Lluch-Cota et al., 2007). El Niño events were defined as at least five consecutive months of MEI.v2 > 0.5, following the National Weather Service Climate Prediction Center (https://origin.cpc.ncep.noaa.gov). The end of an El Niño event was defined as the first

subsequent month with MEI.v2 < 0.5. Duration in months after the end of an El Niño event was included as an environmental covariate to examine whether the effects of El Niño were sustained beyond the duration of the climatic event itself. Data collected on cruises during El Niño events (March 2010 and June 2016, Table S1), were assigned a value of zero months since the end of the previous El Niño.

2.4. Model fitting and selection protocols

Generalized additive models (GAMs) were fit using restricted maximum likelihood parameter estimation (REML) in the *mgcv* package in R (Wood, 2011) to explore the relationship between NASC and environmental conditions. Time in months since the end of the previous El Niño event was included as a covariate in all candidate GAMs. All possible models with single SST (0, 3-, or 12-month average), MEI.v2 (9- or 12-month average) and Chl-*a* (3- or 6-month average) terms were explored (Table 2).

A spatial interaction term (thin plate spline of longitude and latitude) was included to account for expected spatial variability in midtrophic community composition across the diverse regions of our study area and to account for spatial autocorrelation between adjacent datapoints. Residual spatial autocorrelation was examined using Moran's I (Dormann et al., 2007) in the *spdep* package (Bivand and Piras, 2015), and adding a spatial interaction term reduced the spatial autocorrelation of model residuals (Moran's I, decreased from 0.12 to 0.10 at 1 km lag, Fig. S2).

Covariates within each candidate model were examined for collinearity using Pearson's correlation in the *corrplot* package (Wei and Simko, 2017). Residuals of all models of log-transformed NASC were normally distributed, thus Gamma distributions with identity link functions were used for smoothing parameter estimations. Automatic term selection was

282 performed in *mgcv* for all models using "double penalty" shrinkage as described in Marra and
283 Wood (2011). Model selection was performed by comparing second order Akaike Information
284 Criterion (AICc) among candidate models in the *AICcmodavg* package (Mazerolle, 2020).
285 GAMs with spatial interaction terms fit using REML were also used to describe
286 potentially non-linear relationships between metrics of acoustic backscatter and the vertical
287 distribution of backscatter in the upper 200 m of the water column. The effects of wNASC on
288 layer width and the effects of total NASC on the density of scattering layers were examined
289 using Gamma distributions for smoothing parameter estimation with log- and identity-link
290 functions respectively.
291

Table 1.

List of candidate GAM models and results of model selection by second order Akaike Information Criterion (AICc). All models include time in months since the end of the previous El Niño event (moEND) and a thin plate spline of the interaction between longitude and latitude ("s(lon, lat, bs = "tp")"). A single term of NOAA's Multivariate ENSO Index (MEI.v2), sea surface temperature (SST), and sea surface chlorophyll-*a* concentration (Chl-*a*) were included in each model. "s" denotes that the term was fit with a smooth spline. Subscripts after the environmental terms indicate the number of months prior to acoustic sampling over which the covariate was averaged.

$\log_{10}$**NASC ~** *s*(moEND) + *s*(lon, lat, bs = "tp") +	Δ**AIC$_c$**	**Weight**
$s(MEI_{12}) + s(SST) + s(Chl\text{-}a_6)$	**0**	**1**
$s(MEI_{12}) + s(SST) + s(Chl\text{-}a_3)$	21.29	0
$s(MEI_9) + s(SST) + s(Chl\text{-}a_6)$	32.49	0
$s(MEI_9) + s(SST) + s(Chl\text{-}a_3)$	54.47	0
$s(MEI_{12}) + s(SST_3) + s(Chl\text{-}a_6)$	54.97	0
$s(MEI_9) + s(SST_3) + s(Chl\text{-}a_6)$	82.89	0
$s(MEI_{12}) + s(SST_3) + s(Chl\text{-}a_3)$	146.46	0
$s(MEI_{12}) + s(SST_{12}) + s(Chl\text{-}a_6)$	148.31	0
$s(MEI_{12}) + s(SST_{12}) + s(Chl\text{-}a_3)$	192.78	0
$s(MEI_9) + s(SST_3) + s(Chl\text{-}a_3)$	211.51	0
$s(MEI_9) + s(SST_{12}) + s(Chl\text{-}a_6)$	221.78	0
$s(MEI_9) + s(SST_{12}) + s(Chl\text{-}a_3)$	265.55	0

3. Results

NASC integrated between 10-200 m depth per km was quantified over 9,940 km of cruise track covered at night in waters with sea floor depths ≥ 200 m. Layer width, wNASC, and density were available for 9,931 km. NASC (computed over all of our defined Gulf of California regions) was variable among cruises, with approximately an order of magnitude variability in mean values and over two orders of magnitude of variability among the interquartile ranges (Fig. 4). Log-transformed NASC anomalies were highest (i.e., most positive) during July 2007 (mean ± sd = 0.38 ± 0.34), February 2014 (0.34 ± 0.40), and October 2014 (0.19 ± 0.28, Fig. 4). The most negative anomalies occurred during or shortly after strong El Niño events (March 2010: -0.45 ± 0.38; June 2016: -0.25 ± 0.32; and June 2017: -0.48 ± 0.42; Fig. 4).

These qualitative patterns in NASC variability across our timeseries are relatively consistent among the defined geographical regions (Fig. S3). However, variability in NASC among regions was not more robustly compared due to spatio-temporally heterogenous data among cruises and spatial autocorrelation within cruises. Thus, we focus on quantifying general environmental mechanisms driving gulf-wide variability in NASC.

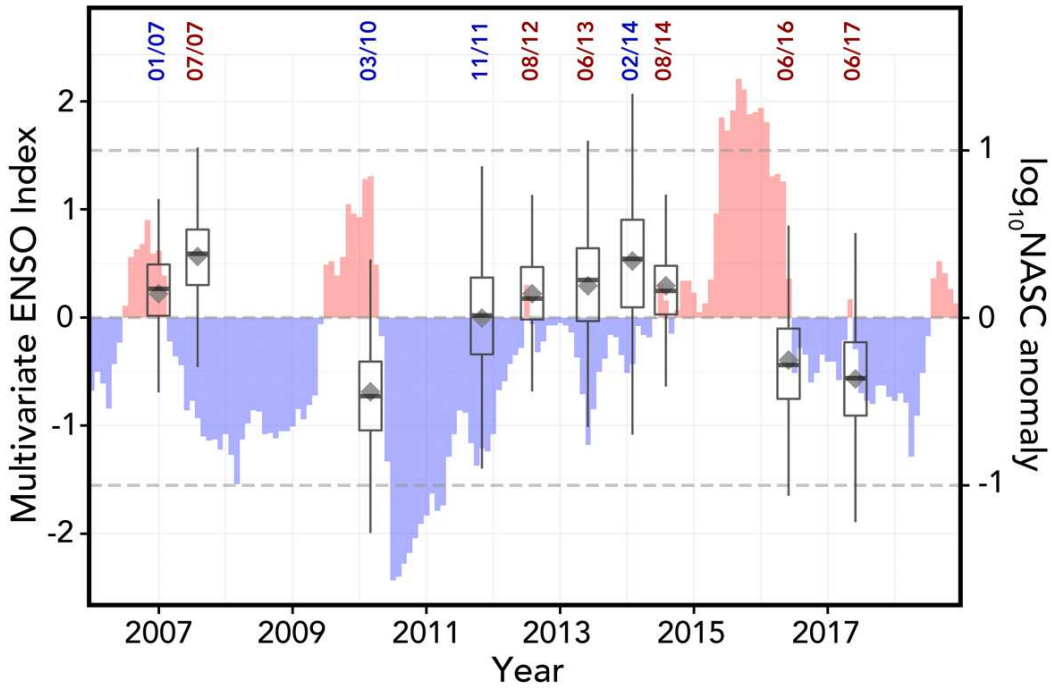

Fig. 4. Relationship between ENSO phase (NOAA's Multivariate ENSO Index v2) and NASC during 2007-2017 represented as boxplots of log-transformed NASC anomalies (deviation from all regional means across our time series) from all ten oceanographic cruises, 2007-2017. Within each boxplot, the mean is represented by a grey diamond and the median as a horizontal black line. Dashed horizontal lines correspond to the $\log_{10}$NASC anomaly axis. Sampling start dates (MM/YY) for the cruises are indicated at the top of the figure and are color coded for warm (red) and cool (blue) sampling periods. Acoustic summaries per cruise are also presented with timeseries of mean monthly sea surface temperature and chlorophyll-*a* concentrations across the study area in Fig. S4, for reference.

3.1. Spatial and environmental effects on acoustic scattering

Standardized model selection based on ΔAIC_c was used determine which temporal averages of MEI.v2, SST, and Chl-*a* best explained variability in NASC in the gulf (Table 1). Most candidate models were comprised of covariates with |Pearson correlation coefficients| < 0.5 (Fig. S5). Our selected model included time in months since the end of the previous El Niño, a spatial interaction term, average SST from the month of collection, average ENSO conditions over the previous 12 months (MEI_{12}), and average Chl-*a* over the previous six months (Table 2, *Adj-*R^2 = 0.42). All environmental covariates in our selected model were minimally correlated (maximum |Pearson correlation coefficient| = 0.53, Fig. S5).

Table 2.

Summary of covariate contributions to the selected generalized additive model of acoustic backscatter in the Gulf of California, Mexico. Coefficient estimates ("estimate"), *t*-values and *p*-values are given for each parametric coefficient. Estimated degrees of freedom (*edf*), *F*-statistics and *p*-values are given for each smooth term ("*s*"). Covariates in the selected model included: time in months since the end of the previous El Niño (moEND); 12-month average MEI.v2 (MEI_{12}); sea surface temperature during the month of collection (SST); average sea surface chlorophyll-*a* concentrations over the previous six months (CHL_6); and a spatial interaction term of longitude and latitude to account for spatial autocorrelation in the data (lon, lat). The maximum allowable number of knots (k) is given for each term.

$log_{10}NASC \sim s(MEI_{12}, k=6) + s(moEND, k=6) + s(SST, k=6) + s(Chl\text{-}a_6, k=6) + s(lon, lat, bs="tp", k=10)$

$Adj.\ R^2 = 0.42$

Parametric coefficients	**estimate**	***t***	***p***
Intercept	2.77	779.1	<< 0.01
Smooth terms	***edf***	***F***	***p***
$s(MEI_{12})$	4.75	350.4	<< 0.01
s(moEND)	4.83	498.9	<< 0.01
s(SST)	4.95	64.2	<< 0.01
$s(Chl\text{-}a_6)$	4.68	19.6	<< 0.01
s(lon, lat)	8.57	33.0	<< 0.01

All environmental covariates included in the selected model explained significant variability in NASC. However, most of the explanatory power could be attributed to the time since the last El Niño ($F = 498.9$, $p << 0.01$), as well as the average MEI.v2 over the 12 months prior to sampling (MEI_{12}; $F = 350.4$, $p << 0.01$, Table 2). La Niña conditions (negative ENSO extremes defined as MEI.v2 < -0.5) had a strong positive effect on backscatter, and increased

MEI_{12} had a strong negative effect on NASC, driving approximately four orders of magnitude of variability across the range of observed MEI_{12} values (Fig. 5B). The negative effect appeared to peak at MEI_{12} > 1.0 and may suggest an upper limit on the possible impact of El Niño conditions, although we only had two observations of MEI_{12} > 1.0 (Fig. 5B).

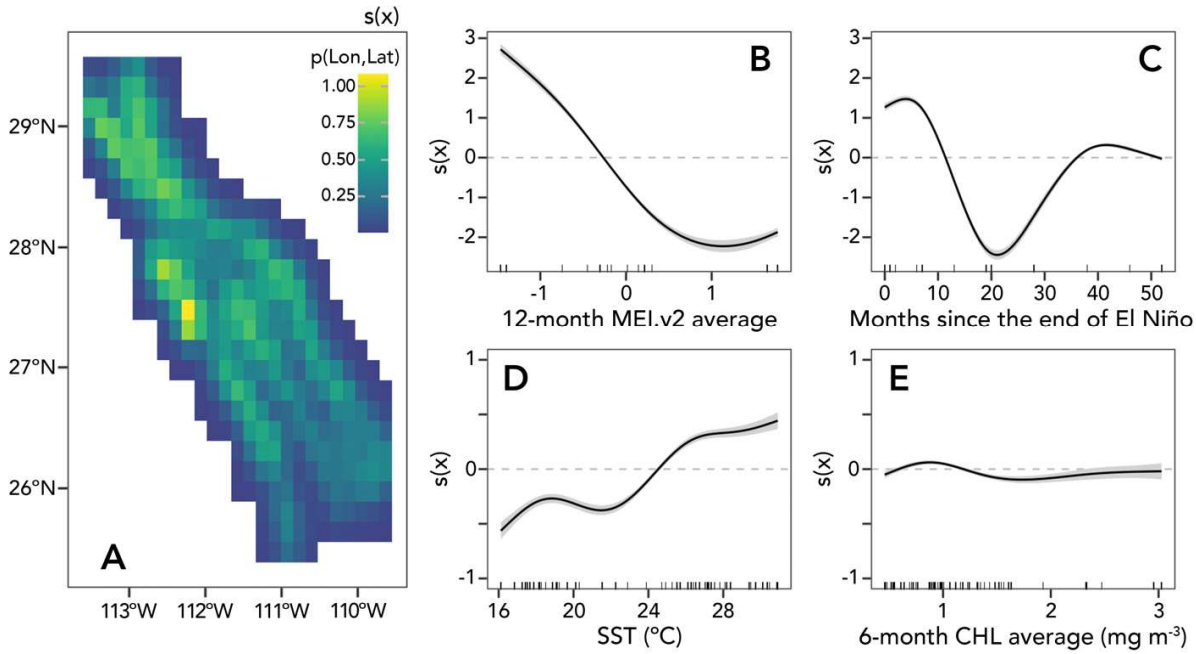

Fig. 5. Partial-effects plots for the environmental covariates in the selected generalized additive model of log_{10}NASC showing the relationship between each covariate and the contribution of the smoother for that covariate to the model's fitted values ("s(x)"). A) Thin plate spline of longitude and latitude; B) 12-month average MEI.v2 (MEI_{12}); C) Time in months since the end of the previous El Niño event (moEND); D) Regional monthly average of sea surface temperature at time of acoustic sampling (SST); E) 6-month average regional sea surface chlorophyll-*a* concentration (CHL_6). In panels B-E, grey shading indicates standard errors about the estimate for each covariate, and rug plots indicate covariate observations.

366 In the first ten months following an El Niño event, there is a decreasing positive effect of
367 time since the end of El Niño on NASC (Fig. 5C), but this turns into a strong negative after ten
368 months, peaking at 24 months, with NASC values being depressed more than 100-fold. The
369 negative effect of an El Niño event thus persists from ~10-36 months following the end of the
370 event, independent of local environmental conditions.
371 Increased SST had a significant positive effect on backscatter, but explained less than one
372 order of magnitude of variability across the entire range of values observed (Table 2, Fig. 5D).
373 The highest SST values are typically observed July-September (Fig. 3), suggesting the effect of
374 SST on acoustic backscatter may at least partially reflect a seasonal signal in local environmental
375 conditions. Although the relationship between CHL_6 and log-transformed NASC was significant,
376 it was largely uninformative and explained little variability across the range of observed values
377 (Table 2, Fig. 5E).
378
379 *3.2. Relationship between NASC, layer width, and density*
380 Integrated NASC within vertically-defined scattering layers (wNASC) was not a useful
381 predictor of the width of those scattering layers in the Gulf of California (GAM, Adj-R^2 =0.05,
382 Table 3, Fig. S6). Width generally increased at the high and low extremes of observed wNASC,
383 but mean width (35.10 ± 19.47 m) remained relatively constant across the most frequently
384 observed values of wNASC (Fig. 6B). However, wNASC explained 75% of variability in layer
385 density (GAM, Table 3, Fig. S6). Scattering layer density increased linearly with NASC during
386 all ten oceanographic cruises, suggesting that as scattering increases, packing density within
387 scattering layers also increases (Fig. 6C).

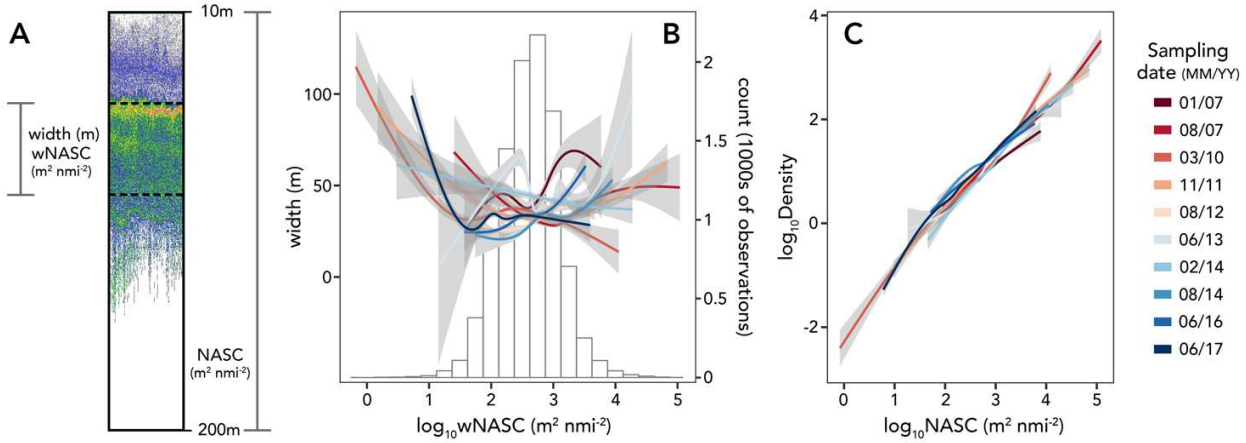

388

389 **Fig. 6.** Relationships between backscatter and the vertical distribution of backscatter per km of
390 cruise track. A) Definitions of width, wNASC, and NASC used for calculating layer density. B)
391 Histogram of log-transformed wNASC observations and its relationship with layer width for
392 each cruise as identified in the inset on the right. C) Relationship between log-transformed layer
393 density (width /wNASC) and log-transformed NASC. Locally estimated scatterplot smooths are
394 given for each cruise and 95% confidence intervals are given as grey bands. Color legend applies
395 to panels B and C.

Table 3.

Summary of covariate contributions models describing the relationship between nighttime backscatter and vertical density distribution in the upper 200 m of the water column in the Gulf of California. Coefficient estimates ("estimate"), *t*-values, and *p*-values are given for each parametric coefficient. Estimated degrees of freedom (*edf*), *F*-statistics, and *p*-values are given for each smooth term ("s"). Definitions of NASC, wNASC, width, and density are provided in the methods and Fig. 2. A spatial interaction term of longitude and latitude was included in each model to account for spatial autocorrelation in the data (lon, lat). The maximum allowable number of knots (k) is given for each term and the adjusted R^2 (*Adj.* R^2) is given for each model.

width ~ s(log₁₀ wNASC, k = 6) + s(lon, lat, bs = "tp", k = 10), Adj. R^2 = 0.05			
Parametric coefficients	**estimate**	***t***	***p***
Intercept	3.55	678.7	<< 0.01
Smooth terms	***edf***	***F***	***p***
s(log₁₀wNASC)	3.90	20.0	<< 0.01
te(lon, lat)	8.31	32.7	<< 0.01

density ~ s(log₁₀ NASC, k = 6) + s(lon, lat, bs = "tp", k = 10), Adj. R^2 = 0.75			
Parametric coefficients	**estimate**	***t***	***p***
Intercept	2.64	688.2	<< 0.01
Smooth terms	***edf***	***F***	***p***
s(log₁₀ NASC)	4.52	14529.6	<< 0.01
te(lon, lat)	8.41	21.1	<< 0.01

4. Discussion

Midtrophic organisms play a central ecological role in open ocean ecosystems, but their responses to seasonal and climatic variability remain poorly understood. We observed variability of backscatter from midtrophic organisms in the central Gulf of California that spanned four orders of magnitude and could largely be explained by ENSO conditions and a seasonal temperature cycle. Although we were not able to directly sample the communities contributing to backscatter during this study, numerous studies indicate that acoustic backscatter at 120 kHz can be mostly attributed to mesozooplankton and micronekton (Domínguez-Contreras et al., 2012; Díaz Santana-Iturríos et al., 2013; Gómez-Gutiérrez et al., 2006; Robinson et al., 2014; García-Fernández et al., this issue). Our observations suggest that the biomass of midtrophic organisms and their contribution to ecosystem function and biogeochemical cycling vary drastically in response to environmental variability.

4.1. Seasonal backscatter variability

Intra-annual variability in NASC was characterized by a positive relationship with SST (Fig. 5), suggesting that backscatter peaks in summer when sea surface temperatures are highest (Hidalgo-González and Alvarez-Borrego, 2004; Kahru et al., 2004) (Fig. 3). Euphausiids, myctophids, sardines, and anchovies often dominate the midtrophic biomass in upwelling systems such as the Gulf of California (Lavaniegos-Espejo and Lara-Lara, 1990; Sánchez-Velasco et al., 2004; Díaz Santana-Iturríos et al., 2013; Ambriz-Arreola et al., 2017; Contreras-Domínguez et al., 2012; Petatán-Ramírez et al., 2019; Weber et al., 2021) and exhibit seasonal breeding cycles that may help explain summer peaks in backscatter as growing individuals become more acoustically visible with increasing size. Brinton and Townsend (1980) reported

April peaks in euphausiid abundance in the central gulf, driven by the neritic species *Nyctiphanes simplex*. Summer peaks in the abundance of larvae and adults of the two most abundant myctophids in our study region, *Benthosema panamense* and *Triphoturus mexicanus*, have been observed during both warm and cool ENSO phases (Aceves-Medina et al., 2004; Díaz Santana-Iturríos et al., 2013).

The sampling frequency and environmental history of our study period limited our ability to robustly describe seasonal variability in backscatter in the Gulf of California (we only made paired warm-cool season samplings in 2007 and 2014). For both paired seasonal sampling events, each characterized by different oceanographic conditions and histories, the variability observed between seasons was orders of magnitude smaller than interannual variability (Fig. 4). The most notable contradictions to the observed summer peaks in backscatter are the abundances of anchovy (*Engraulis mordax*) and sardine (*Sardinops sagax*), which typically peak in cooler months (Contreras-Domínguez et al., 2012; Rubio-Rodríguez et al., 2018; Petatán-Ramírez et al., 2019; Arreguín-Sánchez et al., 2021; Morales-Bojorquez et al., 2021). These fishes are generally more coastal than the dominant euphausiid and myctophid species, which may have also impacted their detectability and inclusion in our analyses. The contributions of anchovy and sardine could be further complicated by commercial fishing pressure, which neither euphausiids nor myctophids experience in the Gulf of California.

Regardless of the complex seasonal dynamics of midtrophic community composition and biomass, impacts of climatic events such as El Niño appear to have a much stronger impact than seasonal cycles on baseline productivity across trophic levels in the Gulf of California. Although the average chlorophyll-*a* concentration over the six months prior to acoustic sampling was not a useful predictor of backscatter, it is possible that we simply did not include this proxy of

phytoplankton biomass at appropriate spatial and temporal resolutions. It is also possible that the spatial interaction term obscured potential effects of phytoplankton biomass on backscatter, as sea surface chlorophyll-*a* concentration was positively correlated with latitude (Fig. S5). Qualitatively, NASC was highest in the Baja Peninsula, Sonora, and Midriff Islands regions (Fig. 1, Fig. S3). These regions exhibit strong seasonal variability in wind- and tidally driven upwelling (Roden, 1964) and experience some upwelling in early summer when the gulf-wide coastal upwelling index is low (Lluch-Cota, 2000). Nutrient enrichment from upwelled waters in these regions may thus support a relatively high biomass of scatterers compared to regions with less upwelling such as the Central Pelagic and Southern regions (Lavaniegos-Espejo and Lara-Lara, 1990; Lluch-Cota, 2000).

4.2. Integrated ENSO conditions largely dictate pelagic acoustic backscatter

Variability in backscatter could largely be explained by ENSO conditions over the twelve months prior to sampling (MEI_{12}, Fig. 5, Table 2). Log-transformed NASC was lowest during or immediately following El Niño events and corresponds to reductions of zooplankton biovolume, as well as euphausiid and larval fish abundances observed in the Gulf of California following the 1982-83, 1997-98, and 2015-16 El Niño events (Lavaniegos et al., 1989; Sánchez-Velasco et al., 2004, García-Fernández et al., this issue).

Changes in backscatter could also reflect variability in midtrophic community composition with ENSO conditions. The relative biomass of gas-bearing organisms (e.g. anchovy, some myctophids and siphonophores) and euphausiids would have the largest impact on the relationship between backscatter at 120 kHz and midtrophic biomass (Lavery et al., 2007; Benoit-Bird and Lawson, 2016). Timeseries describing variability in midtrophic community

composition are limited, but similar responses to ENSO events have been documented for several midtrophic groups in the Gulf of California. Trawl-estimated biomass of fish larvae, euphausiids, and gas-bearing siphonophores all decreased following the 1982-83 El Niño and increased during the subsequent La Niña (Lavaniegos-Espejo and Lara-Lara, 1990; Sánchez-Velasco et al., 2004). Landings of *S. sagax* decreased following the 2009-10 El Niño and landings of *E. mordax* peaked during La Niña conditions in 2013-14 before decreasing during the 2015-16 El Niño (Comisión Nacional de Acuacultura y Pesca, https://datos.gob.mx/busca/dataset/produccion-pesquera). Additionally, Humboldt squid collected from the central gulf following El Niño events consumed more crustaceans and fewer fishes than those collected following ENSO-neutral or La Niña conditions, which could indicate reduced availability of fish prey following El Niño events (Hoving et al., 2013; Portner et al., 2020). Thus, although there have likely been changes in midtrophic community composition during our study period, observed changes in NASC from the central Gulf of California are more likely to reflect changes in total biomass of the midtrophic community.

Changes in the size structure of midtrophic organisms could also affect NASC. However, limited variability in the size of myctophids (~3-4 cm standard length) and enoploteuthid squids (~2 cm mantle length) with ENSO conditions in the diets of Humboldt squid (Portner et al., 2020), suggests that there is limited variability in adult body size of these abundant prey. Thus, we hypothesize that reduced backscatter is indicative of large-scale changes in the pelagic ecosystem of the Gulf of California, likely driven by a combination of changes in the biomass and possibly identity, of midtrophic community constituents in response to local and integrated ENSO conditions.

4.3. Acoustic backscatter is persistently low following El Niño events

Nighttime NASC decreased significantly following El Niño events in 2009-10 and 2015-16 and took two to three years after El Niño ended to recover to values observed prior to the event (Fig. 5C). Our evidence for this pattern of recovery derives primarily from the 2009-10 event, because our dataset ends in June 2017, only one year after the 2015-16 El Niño (Fig. 4). However, qualitative observations from surveys in June 2018 and 2019 suggest a continuation of relatively low backscatter conditions (Robinson and Gómez-Gutiérrez, this issue, *unpublished data*).

The time it takes to recover to pre-El Niño biomass is likely dependent on the generation times of midtrophic organisms and the conditions experienced during the cool (La Niña) and neutral phases of ENSO that follow El Niño events. Some common midtrophic constituents of acoustic scattering layers in the upper 200 m of the Gulf of California, such as euphausiids and small mesopelagic squids, have lifespans of less than one year (Lavaniegos, 1992; Harvey et al., 2010; Ambriz-Arreola et al., 2012, 2017). Fishes such as myctophids and anchovies may mature in as little as a year and reproduce for multiple years (Kawaguchi and Mauchline, 1982; Parrish et al., 1986). If the observed reduction in NASC reflects a decreased abundance of midtrophic organisms following El Niño events, these organisms would require multiple generations to recover to large population sizes, even under favorable environmental conditions. García-Fernandez et al. (this issue) reported that euphausiid abundances in the central Gulf of California during June 2013–2016 were relatively low and took approximately three years following the 2015-16 El Niño to recover to relatively high abundances that characterized historical observations (Brinton and Townsend, 1980).

519 Strong La Niña conditions (MEI.v2 < -1) following El Niño events coincided with the
520 recovery of midtrophic biomass, and thus the entire ecosystem including regional fisheries.
521 Following El Niño 2009-10, strong La Niña conditions persisted for ten months, and mean
522 NASC increased approximately three-fold by the end of 2011, fully recovering to levels
523 observed prior to El Niño by the beginning of 2014 (Fig. 4). Conversely, following El Niño
524 2015-16, La Niña was essentially non-existent, and NASC continued to decrease through mid-
525 2017. It is important to note that 2014 was an unusually warm year in the study region, both in
526 terms of SST and temperature at depth (Frawley et al., 2019; Martínez-Soler et al., 2021), and
527 this phenomenon may have influenced the midtrophic communities prior to El Niño 2015-16
528 and/or further enhanced its effects.
529
530 *4.4. Scattering layer density increases with backscatter*
531 Pelagic fishes and invertebrates engage in complex and dynamic social behaviors, called
532 aggregations, swarms, schools, and shoals (Ritz, 1994; Ritz et al., 2011) that likely modify
533 acoustic density. MVBS within acoustic layers, a proxy for animal density, increased with NASC
534 over a substantial range (Fig. 6C), suggesting that at intermediate spatial scales organisms pack
535 more tightly with their neighbors as the number of individuals increases (Benoit-Bird et al.,
536 2017). For most cruises, the slope of the relationship between density and NASC decreases at
537 relatively high NASC (Fig. 6C), which could indicate an ecologically relevant limiting effect.
538 This pattern, however, may also reflect how our metric of density characterized features with
539 multiple centers of acoustic biomass in the water column. Variability in layer density at higher
540 NASC could be due to more complex acoustic features or multiple acoustic features in the upper

200 m of the water column (Fig. 2C), perhaps composed of species assemblages with different vertical migratory behaviors (Ambriz-Arreola et al., 2017).

A general increase in prey density with increasing backscatter suggests that the accessibility of this midtrophic biomass to the predators it supports increases exponentially. Conversely, reductions in prey biomass could be expected to have non-linear effects on predators as prey density is often more important than overall biomass for a variety of foraging predators, including seabirds (Weimerskirch et al., 2005; Benoit-Bird et al., 2013; Carroll et al., 2017) and rorqual whales (Cade et al., 2021). Effects of environmental variability on predators are thus compounded by changes in both the abundance and distribution of midtrophic prey. It is likely that there were high-density patches of scatterers in our dataset when total NASC was relatively low, but at scales smaller than the resolution of our analyses (Hazen et al., 2009; Benoit-Bird et al., 2019). Examining effects of environmental variability on acoustic backscatter at finer spatial scales than explored in this study would refine our understanding of the effects of climatic variability on midtrophic communities.

4.5. Potential consequences of reduced backscatter from midtrophic communities

Anomalous warming events in the gulf have been more frequent and longer lasting, with two strong El Niño events since 2010 and a pronounced sub-surface warming trend in the 50-150 m depth range between 2006 and 2017 (Frawley et al., 2019). If these patterns of more frequent El Niño events and intervening warming trends continue, it is highly likely that conditions will become increasingly unfavorable to support a large biomass of midtrophic organisms in the Gulf of California (Petatán-Ramírez et al., 2019).

563 A declining trend in standing biomass of midtrophic forage species will negatively
564 impact pelagic predators, and this already appears to have happened in the case of Humboldt
565 squid, at least for individuals of the large phenotype. These squid supported a major fishery until
566 El Niño 2009-10 when squid hatchlings assumed a tropical phenotype characterized by reduced
567 size at maturity, and the fishery collapsed (Hoving et al., 2013; Robinson et al., 2016). A
568 subsequent warming trend flanked by El Niño 2009-10 and 2015-16 has accompanied the
569 persistence of the small phenotype to the present time, and the fishery has reported severely
570 reduced landings since 2010 (Frawley et al., 2019). Thus, the small phenotype replaced the large
571 in the gulf, and while biomass of the small-phenotype stock appeared to remain high until at least
572 2013 (Hoving el al. 2013; Benoit-Bird and Gilly, unpublished data), the current status is unclear.
573 Although subsurface temperature anomalies may directly affect development and maturation of
574 predators in the Gulf of California, our results suggest that temperature also affects the supply of
575 midtrophic organisms that form the diet of many predators in the region, exacerbating direct
576 thermal effects of warming events.
577
578 **5. Conclusions**
579 Perhaps the most ecologically relevant finding of the present study is the approximately
580 three years that may be necessary for midtrophic communities to recover from a strong El Niño
581 event. Increases in the frequency and intensity of El Niño events with global change (Cai et al.,
582 2014, 2015; Jin et al., 2015) could dramatically impact marine ecosystems by limiting the
583 recovery of midtrophic community biomass between El Niño events and result in a chronic,
584 sequential degradation of midtrophic forage, as well as the biomass of predators that depend on
585 this prey resource. Even if La Niña events are also strengthened, the decline in biomass, and

likely overall productivity, of midtrophic communities following El Niño still require multiple generations to recover – a temporal scale that may be longer than the duration of a typical La Niña event. Understanding the drivers and timescales of variability in midtrophic community composition and biomass across diverse marine ecosystems would provide a more refined perspective through which to understand how effects of ocean warming will propagate through oceanic ecosystems.

Declaration of Competing Interest

The authors declare that they have no known competing financial interests or personal relationships that could have appeared to influence the work reported in this paper.

Acknowledgements

We would like to thank the crew of the *R/V El Puma* and the technicians, graduate and undergraduate students, and scientists from the Fisheries Ecology Laboratory, Instituto de Ciencias del Mar y Limnología, Universidad Nacional Autónoma de México (ICMyL-UNAM), Universidad de Guadalajara, Centro de Investigaciones Biológicas del Noroeste (CIBNOR), and Centro Interdisciplinario de Ciencias Marinas (CICIMAR-IPN) for their cooperation in collecting hydroacoustic data. Stephanie Brodie, Gemma Carroll, and Barbara Muhling provided thoughtful feedback on the environmental analyses and generalized additive models. Briony Hutton provided invaluable assistance with the acoustic analyses. The use of the R/V El Puma during the cruises was supported by UNAM, under grants PAPIIT-UNAM IN218106-3, IN2006-10. This research project was funded by DGAPA-PAPIIT UNAM (No. IN200610), CONACYT (Ciencia Básica 2012-152850, FOSEMARNAT-2004-01-C01-144, SAGARPA S007-2005-1-

609 11717, CB-2012-178615-01, CB-2016-01-284201) and El Centro Interdisciplinario de Ciencias
610 Marinas, Instituto Politécnico Nacional (SIP-IPN 2007–2017). C.J.R. and J.G.-G. are SNI
611 fellows. J.G.-G. is also an EDI-IPN and a COFAA-IPN fellow. W.F.G. was supported during the
612 course of this work by grants from the US National Science Foundation (IOS-1557754, OCE-
613 1338973 RAPID, IOS-1420693 EAGER, OCE 0850839, and OCE 0526640), the National
614 Geographic Committee for Research and Exploration (7578-04 and 9366-13), Lindblad
615 Expeditions-National Geographic Fund (LXII-15), and the David and Lucille Packard
616 Foundation (2005-2800 and 32708). K.B.B. was supported by NSF grant 0851239 with
617 additional support from the David and Lucile Packard Foundation through the Monterey Bay
618 Aquarium Research Institute. E.P. was supported in part by the National Science Foundation
619 Graduate Research Fellowship Program under Grant no. DGE-114747 as well as the Esther M.
620 Zimmer Lederberg Trust. The authors have no conflicts of interest to declare.
621

References

Aceves-Medina, G., Jiménez-Rosenberg, S.P.A., Hinojosa-Medina, A., Funes-Rodríguez, R., Saldierna-Martínez, R.J., Smith, P.E., 2004. Fish larvae assemblages in the Gulf of California. J. Fish Biol., 65(3), 832–847. https://doi.org/10.1111/j.1095-8649.2004.00490.x.

Alvarez-Borrego, S., Lara-Lara, J.R., 1991. The physical environment and primary productivity of the Gulf of California: Chapter 26: Part V. Physical oceanography, primary productivity, sedimentology. In M 47: The Gulf and Peninsular Province of the Californias (pp. 555–567). American Association of Petroleum Geologists. http://archives.datapages.com/data/specpubs/history1/images/a114/a1140001/0550/05550.pdf

Ambriz-Arreola, I., Gómez-Gutiérrez, J., Del Carmen Franco-Gordo, M., Lavaniegos, B.E., Godínez-Domínguez, E., 2012. Influence of coastal upwelling-downwelling variability on tropical euphausiid abundance and community structure in the inshore Mexican central Pacific. Mar. Ecol. Prog. Ser., 451, 119–136. https://doi.org/10.3354/meps09607

Ambriz-Arreola, I., Gómez-Gutiérrez, J., Franco-Gordo, M.C., Palomares-García, R.J., Sánchez-Velasco, L., Robinson, C.J., Seibel, B.A., 2017. Vertical pelagic habitat of euphausiid species assemblages in the Gulf of California. Deep-Sea Res. Part I 123, 75–89. https://doi.org/10.1016/j.dsr.2017.03.008.

Arreguín-Sánchez, F., Monte-Luna, P.D., Albañez-Lucero, M.O., Zetina-Rejón, M.J., Tripp-Quezada, A., Ruiz-Barreiro, T.M., Hernández-Padilla, J.C., 2021. How much biomass must remain in the sea after fishing to preserve ecosystem functioning? The case of the

644 sardine fishery in the Gulf of California, Mexico. In Marine Coastal Ecosystems
645 Modelling and Conservation, pp. 143–161. Springer, Cham.
646 Baumgartner, T., Ferreira-Bartrina, V., Schrader, H., Soutar, A., 1985. A 20-year varve record of
647 siliceous phytoplankton variability in the central Gulf of California. Mar. Geol., 64(1–2),
648 113–129. https://doi.org/10.1016/0025-3227(85)90163-X.
649 Benoit-Bird, K.J., 2009. The effects of scattering-layer composition, animal size, and numerical
650 density on the frequency response of volume backscatter. ICES J. Mar. Sci., 66(3), 582–
651 593. https://doi.org/10.1093/icesjms/fsp013.
652 Benoit-Bird, K.J., Au, W.W.L., 2003. Prey dynamics affect foraging by a pelagic predator
653 (*Stenella longirostris*) over a range of spatial and temporal scales. Behav. Ecol.
654 Sociobiol. 53(6), 364–373. https://doi.org/10.1007/s00265-003-0585-4.
655 Benoit-Bird, K.J., Gilly, W., 2012. Coordinated nocturnal behavior of foraging jumbo squid
656 *Dosidicus gigas*. Mar. Ecol. Prog. Ser., 455, 211–228.
657 https://doi.org/10.3354/meps09664.
658 Benoit-Bird, K.J., Battaile, B.C., Heppell, S.A., Hoover, B., Irons, D., Jones, N., Kuletz, K.J.,
659 Nordstrom, C.A., Paredes, R., Suryan, R.M., Waluk, C.M., Trites, A.W., 2013. Prey
660 patch patterns predict habitat use by top marine predators with diverse foraging
661 strategies. PLoS One, 8(1), e53348. https://doi.org/10.1371/journal.pone.0053348.
662 Benoit-Bird, K.J., Lawson, G.L., 2016. Ecological insights from pelagic habitats acquired using
663 active acoustic techniques. Ann. Rev. Ma. Sci., 8(1), 463–490.
664 https://doi.org/10.1146/annurev-marine-122414-034001.

665 Benoit-Bird, K.J., Moline, M.A., Southall, B.L., 2017. Prey in oceanic sound scattering layers
666 organize to get a little help from their friends. Limnol. Oceanogr., 62(6), 2788–2798.
667 https://doi.org/10.1002/lno.10606.
668 Benoit-Bird, K.J., Waluk, C. M., Ryan, J.P., 2019. Forage species swarm in response to coastal
669 upwelling. Geophys. Res. Lett., 46, 1537–1546. https://doi.org/10.1029/2018GL081603.
670 Bivand, R.S., Piras, G., 2015. Comparing implementations of estimation methods for spatial
671 econometrics. J. Stat. Software, 63(18), 1–36. https://doi.org/10.18637/jss.v063. i18.
672 Boyce, D.G., Lewis, M.R., Worm, B., 2010. Global phytoplankton decline over the past century.
673 Nature, 466(7306), 591–596. https://doi.org/10.1038/nature09268.
674 Boyd, P. W., Claustre, H., Levy, M., Siegel, D. A., Weber, T., 2019. Multi-faceted particle
675 pumps drive carbon sequestration in the ocean. Nature, 568(7752), 327–335.
676 https://doi.org/10.1038/s41586-019-1098-2.
677 Brinton, E., Townsend, A. W., 1980. Euphausiids in the Gulf of California—The 1957 cruises.
678 Calif. Coop. Ocean. Fish. Invest. Rep., 21, 211–236.
679 Brinton, E., Fleminger, A., Siegel-Causey, D., 1986. The temperate and tropical planktonic
680 biotas of the Gulf of California. Calif. Coop. Ocean. Fish. Invest. Rep., 27, 228–266.
681 Cade, D.E., Benoit-Bird, K.J., 2015. Depths, migration rates and environmental associations of
682 acoustic scattering layers in the Gulf of California. Deep-Sea Res. Part I, 102, 78–89.
683 https://doi.org/10.1016/j.dsr.2015.05.001.
684 Cade, D. E., Seakamela, S. M., Findlay, K. P., Fukunaga, J., Kahane-Rapport, S. R., Warren, J.
685 D., Calambokidis, J., Fahlbusch, J. A., Friedlaender, A. S., Hazen, E. L., Kotze, D.,
686 McCue, S., Meÿer, M., Oestreich, W. K., Oudejans, M. G., Wilke, C., Goldbogen, J. A.
687 (2021). Predator-scale spatial analysis of intra-patch prey distribution reveals the

688 energetic drivers of rorqual whale super-group formation. Funct. Ecol., 35(4), 894–908.
689 https://doi.org/10.1111/1365-2435.13763.
690 Cai, W., Borlace, S., Lengaigne, M., Van Rensch, P., Collins, M., Vecchi, G., Timmermann, A.,
691 Santoso, A., Mcphaden, M. J., Wu, L., England, M. H., Wang, G., Guilyardi, E., Jin, F.F.,
692 2014. Increasing frequency of extreme El Niño events due to greenhouse warming. Nat.
693 Clim. Change, 4(2), 111–116. https://doi.org/10.1038/nclimate2100.
694 Cai, W., McPhaden, M.J., Santoso, A., Timmermann, A., Jin, F.F., Yeh, S.-W., Takahashi, K.,
695 Vecchi, G., Collins, M., Cobb, KM., Watanabe, M., Wang, G., Lengaigne, M., Wu, L.,
696 An, S.-I., Guilyardi, E., Kug, J.-S., 2015. ENSO and greenhouse warming. Nat. Clim.
697 Change, 5(9), 849–859. https://doi.org/10.1038/nclimate2743.
698 Carroll, G., Cox, M., Harcourt, R., Pitcher, B. J., Slip, D., Jonsen, I., 2017. Hierarchical
699 influences of prey distribution on patterns of prey capture by a marine predator. Funct.
700 Ecol., 31(9), 1750–1760. https://doi.org/10.1111/1365-2435.12873.
701 Chen, Z., Yan, X.-H., Jiang, Y., Jiang, L., 2013. Roles of shelf slope and wind on upwelling: A
702 case study off east and west coasts of the US. Ocean Model., 69, 136–145.
703 https://doi.org/10.1016/j.ocemod.2013.06.004.
704 Choy, C., Wabnitz, C., Weijerman, M., Woodworth-Jefcoats, P., Polovina, J., 2016. Finding the
705 way to the top: How the composition of oceanic mid-trophic micronekton groups
706 determines apex predator biomass in the central North Pacific. Mar. Ecol. Prog. Ser., 549,
707 9–25. https://doi.org/10.3354/meps11680.
708 Croll, D., Marinovic, B., Benson, S., Chavez, F., Black, N., Ternullo, R., Tershy, B., 2005. From
709 wind to whales: Trophic links in a coastal upwelling system. Mar. Ecol. Prog. Ser., 289,
710 117–130. https://doi.org/10.3354/meps289117.

711 Díaz Santana-Iturríos, M., Palacios-Salgado, D.S., Salinas-Zavala, C.A., 2013. Abundance and
712 distribution of lantern fishes (Myctophiformes: Myctophidae) around San Pedro Martir
713 Island, Gulf of California, during 2008. Lat Am. J. Aquat. Res., 41(3), 387–394.
714 https://doi.org/10.3856/vol41-issue3-fulltext-2.
715 Domínguez-Contreras, J.F., Robinson, C.J., Gómez-Gutiérrez, J., 2012. Hydroacoustical survey
716 of near-surface distribution, abundance and biomass of small pelagic fish in the Gulf of
717 California. Pacif. Sci., 66(3), 311–326. https://doi.org/10.2984/66.3.5.
718 Dormann, C.F., McPherson, J.M., Araújo, M.B., Bivand, R., Bolliger, J., Carl, G., Davies, R.G.,
719 Hirzel, A., Jetz, W., Kissling, W.D., Kühn, I., Ohlemüller, R., Peres-Neto, P.R.,
720 Reineking, B., Schröder, B., Schurr, F.M., Wilson, R., 2007. Methods to account for
721 spatial autocorrelation in the analysis of species distributional data: A review. Ecography,
722 30(5), 609–628. https://doi.org/10.1111/j.2007.0906-7590.05171.x.
723 Ducklow, H.W., Steinberg, D.K., Buesseler, K.O., 2001. Upper ocean carbon export and the
724 biological pump. Oceanography, 14(4), 50–58.
725 Echoview Software Pty Ltd, 2019. Echoview® version 10. Echoview Software Pty Ltd, Hobart,
726 Australia.
727 FAO, 2016. The State of World Fisheries and Aquaculture (SOFIA) | FAO | Food and
728 Agriculture Organization of the United Nations. https://doi.org/92-5-105177-1.
729 Faria, J., Jelihovschi, E., Allaman, I., 2018. Conventional Tukey Test. Version 1.3–0. R package.
730 Frawley, T.H., Briscoe, D. K., Daniel, P.C., Britten, G.L., Crowder, L.B., Robinson, C.J., Gilly,
731 W.F., 2019. Impacts of a shift to a warm-water regime in the Gulf of California on jumbo
732 squid (*Dosidicus gigas*). ICES J. Mar. Sci., 76(7), 2413–2426.
733 https://doi.org/10.1093/icesjms/fsz133.

García-Fernández, F., Gómez-Gutiérrez, J., Haskpiel-Segura, C., Ambriz-Arreola, I., De Silva-Dávila, R., Martínez-López, A., Sánchez-Uvera, A., Hernández-Rivas, M., Robinson, C.J., this issue. Interannual spring-summer transition response of euphausiid community abundance during a prolonged anomalous warming in the Gulf of California (2013–2019). Prog. Oceanogr.

Gleckler, P.J., Durack, P.J., Stou, R.J., Johnson, G.C., Forest, C.E., 2016. Industrial-era global ocean heat uptake doubles in recent decades. Nature Clim. Change, 6, 394–398. https://doi.org/10.1038/NCLIMATE2915.

Godø, O.R., Handegard, N.O., Browman, H.I., Macaulay, G.J., Kaartvedt, S., Giske, J., Ona, E., Huse, G., Johnsen, E., 2014. Marine ecosystem acoustics (MEA): Quantifying processes in the sea at the spatio-temporal scales on which they occur. ICES J. Mar. Sci., 71(8), 2357–2369. https://doi.org/10.1093/icesjms/fsu116.

Gómez-Gutiérrez, J., Robinson, C.J., 2006. Tidal current transport of epibenthic swarms of the euphausiid *Nyctiphanes simplex* in a shallow, subtropical bay on Baja California peninsula, México. Mar. Ecol. Prog. Ser., 320, 215–231. https://doi.org/10.3354/meps320215.

Harvey, H. R., Ju, S. J., Son, S.K., Feinberg, L.R., Shaw, C.T., Peterson, W.T., 2010. The biochemical estimation of age in Euphausiids: Laboratory calibration and field comparisons. Deep-Sea Res. Part II: Top. Studies Oceanog., 57(7–8), 663–671. https://doi.org/10.1016/j.dsr2.2009.10.015.

Hazen, E.L., Craig, J.K., Good, C.P., Crowder, L.B., 2009. Vertical distribution of fish biomass in hypoxic waters on the Gulf of Mexico shelf. Mar. Ecol. Prog. Ser., 375, 195–207. https://doi.org/10.3354/meps07791.

757 Hazen, E.L., Johnston, D.W., 2010. Meridional patterns in the deep scattering layers and top
758 predator distribution in the central equatorial Pacific. Fish. Oceanogr., 19(6), 427–433.
759 https://doi.org/10.1111/j.1365-2419.2010.00561.x.
760 Hazen, E.L., Jorgensen, S., Rykaczewski, R.R., Bograd, S.J., Foley, D.G., Jonsen, I.D., Shaffer,
761 S.A., Dunne, J.P., Costa, D.P., Crowder, L.B., Block, B.A., 2013. Predicted habitat shifts
762 of Pacific top predators in a changing climate. Nature Clim. Change, 3(3), 234–238.
763 https://doi.org/10.1038/nclimate1686.
764 Herrera-Cervantes, H., Lluch-Cota, D.B., Lluch-Cota, S.E., Gutie, G., 2007. The ENSO
765 signature in sea-surface temperature in the Gulf of California. J. Mar. Res., 65(5), 589–
766 605. https://doi.org/10.1357/002224007783649529.
767 Hidaka, K., Kawaguchi, K., Murakami, M., Takahashi, M., 2001. Downward transport of
768 organic carbon by diel migratory micronekton in the western equatorial Pacific: Its
769 quantitative and qualitative importance. Deep Sea Res. Part I: Oceanog. Res. Papers
770 48(8), 1923–1939. https://doi.org/10.1016/S0967-0637(01)00003-6.
771 Hidalgo-González, R.M., Alvarez-Borrego, S., 2004. Total and new production in the Gulf of
772 California estimated from ocean color data from the satellite sensor SeaWIFS. Deep Sea
773 Res. Part I: Oceanog. Res. Papers, 51, 739–752.
774 https://doi.org/10.1016/j.dsr2.2004.05.006.
775 Hoving, H.-J.T., Gilly, W.F., Markaida, U., Benoit-Bird, K.J., Brown, Z.W., Daniel, P., Field, J.
776 C., Parassenti, L., Liu, B., Campos, B., 2013. Extreme plasticity in life-history strategy
777 allows a migratory predator (jumbo squid) to cope with a changing climate. Global
778 Change Biol., 19(7), 2089–2103. https://doi.org/10.1111/gcb.12198.

779 Irigoien, X., Klevjer, T.A., Røstad, A., Martinez, U., Boyra, G., Acuña, J. L., Bode, A.,
780 Echevarria, F., Gonzalez-Gordillo, J. I., Hernandez-Leon, S., Agusti, S., Aksnes, D.L.,
781 Duarte, C.M., Kaartvedt, S., 2014. Large mesopelagic fishes biomass and trophic
782 efficiency in the open ocean. Nature Comm., 5, 3271
783 https://doi.org/10.1038/ncomms4271.
784 Jin, F.-F., England, M.H., Takahashi, K., Cai, W., Collins, M., Guilyardi, E., Santoso, A.,
785 Timmermann, A., Lengaigne, M., Vecchi, G., Dommenget, D., Wang, G., Wu, L.,
786 McPhaden, M.J., 2015. Increased frequency of extreme La Niña events under greenhouse
787 warming. Nature Clim. Change, 5(2), 132–137. https://doi.org/10.1038/nclimate2492.
788 Kahru, M., Marinone, S. G., Lluch-Cota, S.E., Pares-Sierra, A., Mitchell, B.G., 2004. Ocean-
789 color variability in the Gulf of California: Scales from days to ENSO. Deep-Sea Res. II,
790 51, 139–146. https://doi.org/10.1016/j.dsr2.2003.04.001.
791 Kawaguchi, K., Mauchline, J., 1982. Biology of Myctophid fishes (Family Myctophidae) in the
792 Rockall Trough, Northeastern Atlantic Ocean. Biol. Oceanogr., 1(4), 337–373.
793 https://doi.org/10.1080/01965581.1982.10749447.
794 Keith, G.J., Ryan, T.E., Kloser, R.J., 2005. ES60adjust. jar. Java software utility to remove a
795 systematic error in Simrad ES60 data. CSIRO Marine and Atmospheric Research,
796 Castray Esplanade, Hobart, Tasmania, Australia.
797 Klevjer, T.A., Irigoien, X., Røstad, A., Fraile-Nuez, E., Benítez-Barrios, V.M., Kaartvedt, S.,
798 2016. Large scale patterns in vertical distribution and behaviour of mesopelagic
799 scattering layers. Sci. Rep., 6, 19873. https://doi.org/10.1038/srep19873.

800 Kloser, R.J., Ryan, T.E., Young, J.W., Lewis, M.E., 2009. Acoustic observations of micronekton
801 fish on the scale of an ocean basin: Potential and challenges. ICES J. Mar. Sci., 66, 998–
802 1006. https://doi.org/10.1093/icesjms/fsp077.
803 Koslow, J.A., Davison, P., Ferrer, E., Jiménez-Rosenberg, S.P.A., Aceves-Medina, G., Watson,
804 W., 2018. The evolving response of mesopelagic fishes to declining midwater oxygen
805 concentrations in the southern and central California Current. ICES J. Mar. Sci. 76(3),
806 626–638. https://doi.org/10.1093/icesjms/fsy154.
807 Lavaniegos, B.E., Lara-Lara, J.R., Brinton, E., 1989. Effects of the 1982-83 El Niño event on the
808 Euphausiid populations of the Gulf of California. Calif. Coop. Ocean. Fish. Invest. Rep.,
809 30, pp. 73–87.
810 Lavaniegos-Espejo, B.E., Lara-Lara, J.R., 1990. Zooplankton of the Gulf of California Mexico
811 after the 1982 To 1983 El Niño event biomass distribution and abundance. Pacif. Sci.,
812 44(3), pp. 297–310.
813 Lavery A.C., Wiebe P.H., Stanton T.K., Lawson G.L., Benfield M.C., Copley N.C., 2007.
814 Determining dominant scatterers of sound in mixed zooplankton populations. J. Acoust.
815 Soc. Am., 122, 3304–3326. https://doi.org/10.1121/1.2793613.
816 Levitus, S., Antonov, J.I., Wang, J., Delworth, T.L., Dixon, K.W., Broccoli, A.J., 2001.
817 Anthropogenic warming of Earth's climate system. Science, 292, 267–271.
818 https://doi.org/10.1126/science.1058154.
819 Lewison, R.L., Crowder, L.B., Read, A.J., Freeman, S.A., 2004. Understanding impacts of
820 fisheries bycatch on marine megafauna. TREE, 19(11), 598–604.
821 https://doi.org/10.1016/j.tree.2004.09.004.

822 Lluch-Cota, S.E., 2000. Coastal upwelling in the eastern Gulf of California. Oceanol. Acta,
823 23(6), 731–740. https://doi.org/10.1016/S0399-1784(00)00121-3.
824 Lluch-Cota, S.E., Aragón-Noriega, E.A., Arreguín-Sánchez, F., Aurioles-Gamboa, D., Jesús
825 Bautista-Romero, J., Brusca, R.C., Cervantes-Duarte, R., Cortés-Altamirano, R., Del-
826 Monte-Luna, P., Esquivel-Herrera, A., Fernández, G., Hendrickx, M.E., Hernández-
827 Vázquez, S., Herrera-Cervantes, H., Kahru, M., Lavín, M., Lluch-Belda, D., Lluch-Cota,
828 D.B., López-Martínez, J., Sierra-Beltrán, A.P., 2007. The Gulf of California: Review of
829 ecosystem status and sustainability challenges. Prog. Oceanogr., 73(1), 1–26.
830 https://doi.org/10.1016/j.pocean.2007.01.013.
831 Lluch-Cota, S.E., Parés-Sierra, A., Magaña-Rueda, V.O., Arreguín-Sánchez, F., Bazzino, G.,
832 Herrera-Cervantes, H., Lluch-Belda, D., 2010. Changing climate in the Gulf of
833 California. Prog. Oceanogr., 87(1–4), 114–126.
834 https://doi.org/10.1016/j.pocean.2010.09.007.
835 MacLennan, D.N., Fernandes, P.G., Dalen, J., 2002. A consistent approach to definitions and
836 symbols in fisheries acoustics. ICES J. Mar. Sci., 59(2), 365–369.
837 https://doi.org/10.1006/jmsc.2001.1158.
838 Marra, G., Wood, S.N., 2011. Practical variable selection for generalized additive models. Comp.
839 Stat. Data Anal., 55(7), 2372–2387. https://doi.org/10.1016/j.csda.2011.02.004.
840 Martínez-Soler, E., Gómez-Gutiérrez, J., De Silva-Dávila, R., González-Rodríguez, E., Aburto-
841 Oropeza, O., 2021. Cephalopod paralarval species richness, abundance, and size structure
842 during the 2014–2017 anomalous warm period in the southern Gulf of California. J.
843 Plankton Res. 43, 224–243. https://doi.org/10.1093/plankt/fbab010.

844 Mazerolle, M.J., 2020. AICcmodavg: Model selection and multimodel inference based on
845 (Q)AIC(c). https://cran.r-project.org/package=AICcmodavg.
846 McClatchie, S., Dunford, A., 2003. Estimated biomass of vertically migrating mesopelagic fish
847 off New Zealand. Deep-Sea Res. Part I: Oceanogr. Res. Pap., 50(10–11), 1263–1281.
848 https://doi.org/10.1016/S0967-0637(03)00128-6.
849 Morales-Bojórquez, E., Nevárez-Martínez, M. O., García-Alberto, G., Villalobos, H., Aguirre-
850 Villaseñor, H., Larios-Castro, E., González-Peláez, S.S., Arizmendiz-Rodríguez, D.I.,
851 Martínez-Zavala, M.Á., 2021. Interaction between marine fauna and the small pelagic
852 fishery in the coastal environment of the Gulf of California, Mexico. Front. Mar. Sci., 8,
853 685. https://doi.org/10.3389/fmars.2021.669176.
854 Parrish, R.H., Mallicoate, D.L., Klingbeil, R.A., 1986. Age dependent fecundity, number of
855 spawnings per year, sex ratio, and maturation stages in northern anchovy, *Engraulis*
856 *mordax*. Fish. Bull., 84(3), 503–517.
857 Petatán-Ramírez, D., Ojeda-Ruiz, M. Á., Sánchez-Velasco, L., Rivas, D., Reyes-Bonilla, H.,
858 Cruz-Piñón, G., Mozaira-Luna, H.N., Cisneros-Montemayor, A.M., Cheung, W.,
859 Salvadeo, C., 2019. Potential changes in the distribution of suitable habitat for Pacific
860 sardine (*Sardinops sagax*) under climate change scenarios. Deep Sea Res. Part II: Top.
861 Stud. Oceanogr., 169, 104632. https://doi.org/10.1016/j.dsr2.2019.07.020.
862 Polovina, J.J., Howell, E.A., Abecassis, M., 2008. Ocean's least productive waters are
863 expanding. Geophys. Res. Lett., 35, L03618. https://doi.org/10.1029/2007GL031745.
864 Polovina, J.J., Abecassis, M.A., Howell, E.A., Woodworth, P., 2009. Increases in the relative
865 abundance of mid-trophic levels fishes concurrent with declines in apex predators in the
866 subtropical North Pacific, 1996-2006. Fish. Bull., 107(4), 523–531.

867 Portela, E., Beier, E., Barton, E.D., Castro, R., Godínez, V., Palacios-Hernández, E., Trasviña,
868 A., 2016. Water masses and circulation in the tropical Pacific off central Mexico and
869 surrounding areas. J. Physical Oceanogr. 46, 3069–3081. https://doi.org/10.1175/JPO-D-16-
870 0068.1.
871 Portner, E.J., Markaida, U., Robinson, C.J., Gilly, W.F., 2020. Trophic ecology of Humboldt
872 squid, *Dosidicus gigas*, in conjunction with body size and climatic variability in the Gulf
873 of California, Mexico. Limnol. Oceanogr., 65, 732–748.
874 https://doi.org/10.1002/lno.11343.
875 Proud, R., Cox, M.J., Brierley, A.S., 2017. Biogeography of the Global Ocean's mesopelagic
876 zone. Current Biol., 27(1), 113–119. https://doi.org/10.1016/j.cub.2016.11.003.
877 R Core Team, 2020. R: A language and environment for statistical computing. R Foundation for
878 Statistical Computing. Vienna, Austria.
879 Ritz, D.A., 1994. Social aggregation in pelagic invertebrates. Adv. Mar. Biol., 30, 155–216.
880 https://doi.org/10.1016/S0065-2881(08)60063-2.
881 Ritz, D.A., Hobday, A.J., Montgomery, J.C., Ward, A.J., 2011. Social aggregation in the pelagic
882 zone with special reference to fish and invertebrates. Adv. Mar. Biol., 60, 161227.
883 https://doi.org/10.1016/B978-0-12-385529-9.00004-4.
884 Robinson, C.J., Avilés-Díaz, L., Gómez-Gutiérrez, J., Salinas-Zavala, C., Camarillo-Coop, S.,
885 Mejia-Rebollo, A., 2014. Hydroacoustic survey of the jumbo squid *Dosidicus gigas* in the
886 Gulf of California during March and September-October 2010. Hidrobiológica, 24(1),
887 39–49.
888 Robinson, C.J., Gómez-Gutiérrez, J., Markaida, U., Gilly, W.F., 2016. Prolonged decline of
889 jumbo squid (*Dosidicus gigas*) landings in the Gulf of California is associated with

chronically low wind stress and decreased chlorophyll-*a* after El Niño 2009-2010. Fish. Res. 173(2), 128–138. https://doi.org/10.1016/j.fishres.2015.08.014.

Robison, B.H., 1972. Distribution of the midwater fishes of the Gulf of California. Copeia, 1972(3), 448–461.

Roden, G.I., 1964. Oceanographic Aspects of Gulf of California1. In T. H. van Andeld Jr. Shor George G. (Eds.), Marine Geology of the Gulf of California: A symposium. Amer. Ass. Petrol. Geol. https://doi.org/10.1306/M3359C2.

Round, F.E., 1967. The phytoplankton of the Gulf of California. Part I. Its composition, distribution and contribution to the sediments. J. Exp. Mar. Biol. Ecol., 1(1), 76–97. https://doi.org/10.1016/0022-0981(67)90008-1.

Rubio-Rodríguez, U., Villalobos, H., Nevárez-Martínez, M.O., 2018. Acoustic observations of the vertical distribution and latitudinal range of small pelagic fish schools in the Midriff Islands Region, Gulf of California, Mexico. Lat. Amer. J. Aquat. Res., 46(5), 989–1000. http://dx.doi.org/10.3856/vol46-issue5-fulltext-12.

Rykaczewski, R.R., Dunne, J.P., 2011. A measured look at ocean chlorophyll trends. Nature, 472, E5. https://doi.org/10.1038/nature09952.

Sánchez-Velasco, L., Avalos-García, C., Rentería-Cano, M., Shirasago, B., 2004. Fish larvae abundance and distribution in the central Gulf of California during strong environmental changes (1997–1998 El Niño and 1998–1999 La Niña). Deep Sea Res. Part II: Top. Studies Oceanogr., 51(6), 711–722. https://doi.org/10.1016/j.dsr2.2004.05.021.

Schukat, A., Bode, M., Auel, H., Carballo, R., Martin, B., Koppelmann, R., Hagen, W., 2013. Pelagic decapods in the northern Benguela upwelling system: Distribution,

912 ecophysiology and contribution to active carbon flux. Deep Sea Res. Part I: Oceanogr.
913 Res. Pap., 75, 146–156. https://doi.org/10.1016/j.dsr.2013.02.003.
914 Staines-Urías, F., Douglas, R. G., Gorsline, D.S., 2009. Oceanographic variability in the southern
915 Gulf of California over the past 400 years: Evidence from faunal and isotopic records
916 from planktic foraminifera. Palaeogeogr., Palaeoclimatol., Palaeoecol., 284(3–4), 337–
917 354. https://doi.org/10.1016/j.palaeo.2009.10.016.
918 Veit, R.R., McGowan, J.A., Ainley, D.G., Wahl, T.R., Pyle, P., 1997. Apex marine predator
919 declines ninety percent in association with changing oceanic climate. Global Change
920 Biol., 3(1), 23–28. https://doi.org/10.1046/j.1365-2486.1997.d01-130.x.
921 Velarde, E., Ezcurra, E. Anderson, D., 2013. Seabird diets provide early warning of sardine
922 fishery declines in the Gulf of California. Sci. Rep., 3, 1332.
923 https://doi.org/10.1038/srep01332.
924 Velarde, E., Ezcurra, E., Horn, M.H., Patton, R.T., 2015. Warm oceanographic anomalies and
925 fishing pressure drive seabird nesting north. Sci. Adv., 1(5), e1400210.
926 https://doi.org/10.1126/sciadv.1400210.
927 Weber, E.D., Auth, T.D., Baumann-Pickering, S., Baumgartner, T.R., Bjorkstedt, E.P., Bograd,
928 S.J., Burke, B.J., Cadena-Ramírez, J.L., Daly, E.A., de la Cruz, M., Dewar, H., Field, J.
929 C., Fisher, J.L., Giddings, A., Goericke, R., Gomez-Ocampo, E., Gomez-Valdes, J.,
930 Hazen, E.L., Hildebrand, J., Zeman, S.M., 2021. State of the California Current 2019–
931 2020: Back to the future with marine heatwaves? Front. Mar. Sci., 8, 709454.
932 https://doi.org/10.3389/fmars.2021.709454.
933 Wei, T., Simko, V., 2017. R package "corrplot": Visualization of a Correlation Matrix (Version
934 0.84). Available from https://github.com/taiyun/corrplot.

935 Weimerskirch, H., Gault, A., Cherel, Y., 2005. Prey distribution and patchiness: Factors in
936 foraging. Ecology, 86(10), 2611–2622. https://doi.org/10.1890/04-1866.
937 Wolter, K., Timlin, M.S., 1993. Monitoring ENSO in COADS with a Seasonally Adjusted
938 Principal Component Index. Proceedings of the 17th Climate Diagnostics Workshop, 52–
939 57.
940 Wood, S., 2011. Fast stable restricted maximum liklihood and marginal liklihood estimation of
941 semiparametric generalized linear models. J. Royal Stat. Soc. Ser. B, 73(1), 3–36.
942 https://doi.org/10.1111/j.1467-9868.2010.00749.x.
943 Woodworth-Jefcoats, P., Polovina, J., Howell, E., Blanchard, J., 2015. Two takes on the
944 ecosystem impacts of climate change and fishing: Comparing a size-based and a species-
945 based ecosystem model in the central North Pacific. Prog. Oceanogr.
946 https://doi.org/10.1016/j.pocean.2015.04.004.
947 Young, J.W., Hunt, B.P.V, Cook, T.R., Llopiz, J.K., Hazen, E.L., Pethybridge, H.R., Ceccarelli,
948 D., Lorrain, A., Olson, R.J., Allain, V., Menkes, C., Patterson, T., Nicol, S., Lehodey, P.,
949 Kloser, R.J., Arrizabalaga, H., Anela Choy, C., 2015. The trophodynamics of marine top
950 predators: Current knowledge, recent advances and challenges. Deep-Sea Res. Part II:
951 Top. Stud. Oceanogr., 113, 170–187. https://doi.org/10.1016/j.dsr2.2014.05.015.
952 Zhang, X., Dam, H.G., 1997. Downward export of carbon by diel migrant mesozooplankton in
953 the central equatorial Pacific. Deep-Sea Res. II, 44(9–10), 2191–2202.
954 https://doi.org/10.1016/S0967-0645(97)00060-X.
955